

Are Buckyballs Hydrophobic?

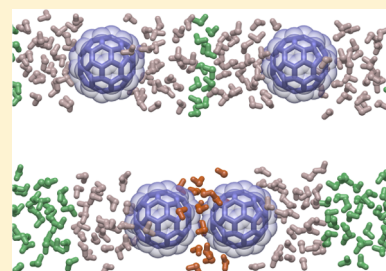
Ronen Zangi*

Department of Organic Chemistry I, University of the Basque Country UPV/EHU, Avenida de Tolosa 72, 20018 San Sebastian, Spain

IKERBASQUE, Basque Foundation for Science, 48013 Bilbao, Spain

S Supporting Information

ABSTRACT: Buckyballs exhibit two seemingly opposing characters. On one hand, they are known to be insoluble in water with all potential chemical properties of being hydrophobic. On the other hand, their pairwise effective interaction in water includes a repulsive solvent-induced contribution. We perform molecular dynamics simulations of the association process of two C_{60} fullerenes in water at different temperatures in order to reconcile these contradicting observations. For comparison, the simulations were also performed in a nonpolar solvent, and the results were further contrasted with those obtained previously for the association of graphene sheets. Considering the association in water, we find small magnitudes for the enthalpy and entropy changes with small positive slopes as a function of temperature, implying an almost negligible change in the heat capacity at constant pressure. These findings sharply contradict the behavior of typical hydrophobic interactions. The reason for these abnormalities, as well as for the repulsive nature of the solvent-induced interactions, is the shape of the contact state that supports the existence of a distinct type of interfacial waters located between two convex surfaces of two buckyballs. These interfacial waters are characterized by smaller entropy and lower density and form a smaller number of hydrogen bonds with surrounding waters compared with those of the interfacial waters around the dissociated solutes. Thus, upon bringing the C_{60} fullerenes into contact, the changes associated with the liberation of the latter to bulk waters are opposed by the concomitant conversion of the latter also to the distinct waters between the two spherical solutes. We argue that although the effective pair interaction is not hydrophobic, the solvation properties are hydrophobic. In the hydration free energy of a single solute, there is no contact state. Furthermore, in the solubility at the macroscopic scale, the relative number of these distinct waters around a large aggregate is smaller, and hence, they are not predicted to influence much the solvation properties. Therefore, buckyballs can serve as an example in which hydrophobic interaction cannot be deduced from hydrophobic solvation.



■ INTRODUCTION

The solubility of C_{60} fullerene in water is very low, whereas it is much higher in nonpolar solvents, especially those that include aromatic rings.^{1,2} In order to increase the solubility in water, derivatives with polar group substituents have been introduced.³ These observations and the nonpolar character of its sole component, the carbon atom, emphatically suggest that C_{60} fullerene is hydrophobic. This inference would not have been granted a second thought without the report by Li et al. on the *repulsive* contribution of the solvent to the effective interaction between two C_{60} fullerenes (hereafter referred to as C_{60} 's, fullerenes, or buckyballs) in water.^{4,5} The finding of their computational study, which was later reproduced independently,⁶ means that the water molecules push two fullerenes away from each other. It clearly contradicts our perception of pairwise hydrophobic interactions in which there is a strong tendency of the surrounding waters to minimize the solvent-exposed surface area of the hydrophobes by pushing them toward each other. How should we then think about buckyballs? Can they be hydrophobic and at the same time attracted to waters more than the waters are attracted to themselves?

The driving force for the association of hydrophobes in aqueous solution depends on their size.⁷ Length-scale depend-

ence arises from the fact that around small solutes, small distortions of the acceptor–hydrogen–donor angle allow the number of hydrogen bonds per water molecule to be similar to that in the bulk.⁸ However, the water layer next to an extended hydrophobic surface cannot maintain its hydrogen bond network, and there is a decrease in the interaction energy between these interfacial waters.⁷ Consequently, the association of two small hydrophobes is driven only by entropy, whereas that of large hydrophobes is driven also by enthalpy.^{9,10} The crossover length between small- and large-scale hydrophobic solvation is about 1 nm. This size is on the order of the diameter of C_{60} , and it has been argued that fullerenes cannot be treated as small or large classical hydrophobic solutes.⁶ It should be emphasized though, that attractive solvent-induced interaction of the potential of mean force (PMF) between two typical hydrophobes is observed, both at the small- and large-scale regimes.

Low solubility is a necessary but not sufficient condition for hydrophobic solvation. How do we then define hydrophobic interaction? There are two thermodynamic signatures that are

Received: August 12, 2014

Revised: September 23, 2014

Published: September 26, 2014

unique for the interactions between hydrophobes.¹¹ The first is the large positive unitary entropy (the measured entropy minus the mixing entropy) change, ΔS_w ,^{12–18} due to restrictions in the orientations of waters¹⁹ and rearrangements of the water–water hydrogen bonds next to the hydrophobes.¹⁰ With increasing temperatures, ΔS_w decreases rapidly and approaches zero at high temperatures.²⁰ The observed negative slope is because at higher temperatures, the entropy of the interfacial waters becomes similar to that of bulk waters. Nonetheless, at the temperature at which ΔS_w vanishes, the interfacial waters are still distinct; they are characterized by a substantial orientational ordering relative to the bulk; however, there is a compensating contribution of translational entropy. The second characteristic of hydrophobic association is the large and negative heat capacity change, ΔC_p , accompanying the process.^{15,21–25} This indicates that also the change in enthalpy is a strong function of temperature with a negative slope. For small solute association, the enthalpy change is positive but changes sign with a temperature increase.²⁶ However, for two large and flat hydrophobic plates, ΔH is negative for all temperatures and strongly and linearly decreases (i.e., increases in magnitude) with T .²⁵ The Gibbs (free) energy for hydrophobic association, ΔG , is characterized by a large and negative value, and despite the strong dependence of the enthalpy and entropy on temperature, it is very weakly temperature-dependent.^{15,25–30} This indicates an almost complete enthalpy–entropy cancellation of their changes with temperature.

What is the molecular picture behind the large and negative ΔC_p characterizing hydrophobic association? On the basis of the observation that (in addition to ΔS_w) the heat capacity change is linearly proportional to the surface area eliminated in the association process, the following view has been suggested.^{22,27,31–34} At low temperature, the ordered water molecules around the solute populate low-energy and low-entropy states. With increasing temperature, the waters surrounding the solute, which form the most fragile hydrogen bonds, increasingly populate higher-energy and higher-entropy states. Thus, at high temperatures, the ordered water structure at the interface “melts”. These two energetic states provide an energy storage mechanism, and as a result, the capacity of the solution to absorb heat is large.

One of the qualitative differences between small- and large-scale hydrophobicity is the occurrence of a drying transition.^{18,35,36} For interplate distances smaller than a critical value, the confined water is thermodynamically unstable in its liquid phase and evaporates. This transition is observed only in superhydrophobic systems but not, for example, in graphene sheets because of the relatively strong solute–water interactions.^{10,37} Although they differ by shape, but are nevertheless chemically similar, C_{60} 's do not exhibit the drying transition.³⁸ However, shape does matter, as evidenced, for example, by the attractive solvent-induced interaction between graphene sheets.¹⁰ Wallqvist and Berne were the first to argue that the curvature of the hydrophobic solute influences its solvation free energy.³⁹ This put into question the ill-practice of blindly multiplying the solvent-accessible surface area by a constant (representing free energy per unit area) to estimate the free energy of hydrophobic hydration. More specifically, they found that a hydrophobic oblate ellipsoid will be more soluble in water than a hydrophobic sphere of the same surface area. If we apply these results obtained from hydrophobic solvation to hydrophobic interaction for buckyballs and graphene sheets, we will arrive at the conclusion that because graphene sheets are

predicted to be more soluble (because they are more oblate than spherical), their pairwise effective attraction should be weaker. In addition, the water-induced interactions between two fullerenes should have a stronger contribution for driving them into contact. This is clearly not the case, and it is one of the purposes of this work to demonstrate that hydrophobic solvation and hydrophobic interaction are not always the reciprocal of each other. What is missing in the picture of solvation are the properties of the dimeric state that in some cases cannot be extrapolated from that of the monomeric state.

In this paper, we perform molecular dynamics (MD) simulations to investigate the pairwise effective interactions between two C_{60} molecules in water. For comparison with the behavior in nonpolar solvents, we also repeat the simulations in *n*-hexane. In addition, we also contrast the results found in water with that of the association of graphene sheets with different sizes.¹⁰ Our results confirm the repulsive nature of the solvent-induced interaction between fullerenes in water. We find that the changes in enthalpy and entropy, as well as their temperature dependence, exhibit abnormal behavior relative to those observed for typical hydrophobic interactions. In particular, the change in the heat capacity at constant pressure is predicted to be very small. The reasons for these peculiarities are the properties of the associated state of two buckyballs. In this dimeric state, a new type of interfacial waters, located between two convex surfaces of the two fullerenes, is introduced. These waters are characterized by a smaller number of water–water hydrogen bonds and a smaller entropy compared with those of the interfacial waters around the monomeric state. We argue that despite this unusual behavior in the pairwise effective interaction between two C_{60} 's, the macroscopic behavior, in which large aggregates are in equilibrium with individually solvated species, might not be too different from that of classical hydrophobic solvation because the spaces between two convex surfaces in the interior of the aggregates will be dry.

METHODS

We performed MD simulations to study the nature of the pairwise effective interaction between two Buckminsterfullerenes in water. The computational details are similar to those applied in our previous work studying the hydrophobic interactions between graphene sheets at different length scales.¹⁰ In particular, the carbon–water interactions and the water model are the same, permitting direct comparison between the two studies. The carbon–water Lennard-Jones (LJ) parameters, $\sigma_{CO} = 0.319$ nm and $\epsilon_{CO} = 0.392$ kJ/mol, were taken from parametrization of the contact angle of water on graphite.⁴⁰ These values were also used to extract the LJ parameters (using the geometric combination rule) between two carbon atoms. During simulations, the positions of the buckyball's atoms were held fixed, and the interactions between atoms on the same fullerene were excluded. The two buckyballs approached each other via their pentagon rings orientated in parallel and out of registry. We used the MD package GROMACS version 4.0.5⁴¹ to perform all of the computer simulations with a time step of 0.002 ps. The electrostatic forces were evaluated by the Particle-Mesh Ewald method⁴² (with a real-space cutoff of 1.0 nm, grid spacing of 0.12 nm, and quadratic interpolation) and the LJ forces by a cutoff of 1.0 nm (with long-range dispersion corrections for the energy and pressure). The system was maintained at a constant temper-

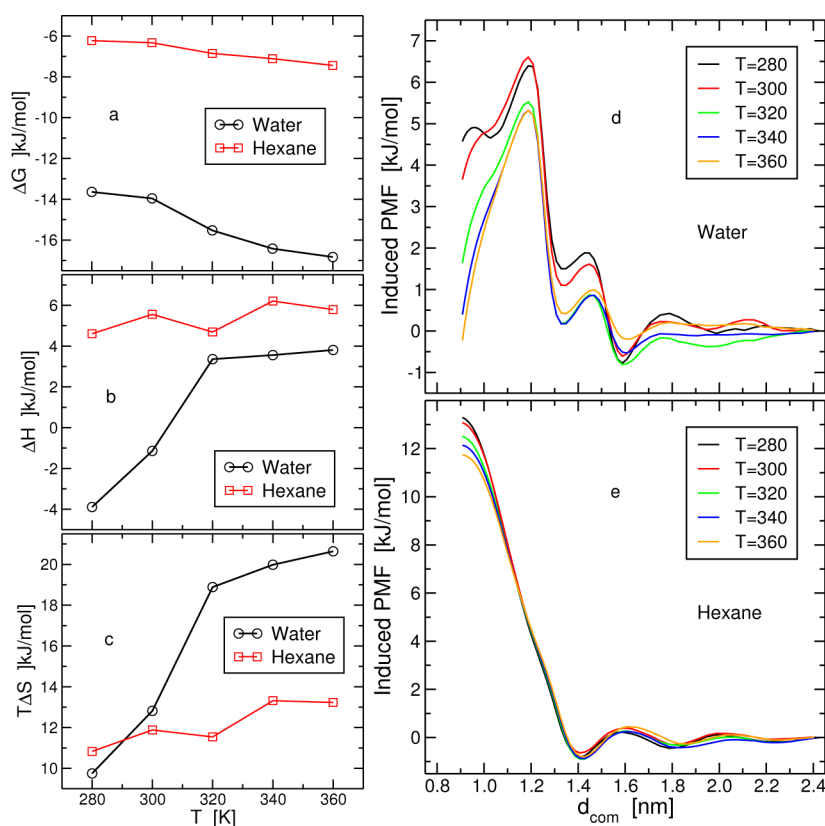


Figure 1. (a) The total free energy change, ΔG , for the association of two fullerenes in water and in hexane as a function of temperature. (b,c) Decomposition of ΔG to its changes in (total) enthalpy and entropy, respectively. (d,e) The solvent-induced PMF between the two fullerenes as a function of the distance between their centers of mass in water and in hexane, respectively.

ature by the velocity rescaling thermostat⁴³ and at a pressure of 1.0 bar by the Berendsen thermostat.⁴⁴

The buckyballs were placed in a rectangular box in which the box lengths along the x and y axes were equal to and smaller than that along the z -axis. The simulation box was filled by 1282 water molecules described by the TIP4P-Ew model⁴⁵ (see Figure S1 in the Supporting Information for snapshots). Their bond distances and angle were constrained using the SETTLE algorithm.⁴⁶ In a separate set of simulations, we dissolved the buckyballs in a nonpolar solvent. To this end, we used 195 n -hexane molecules described by an improved GROMOS96 (43A2) model.⁴⁷ In this case, the bonds between the carbon atoms of n -hexane were constrained using the LINCS algorithm.⁴⁸

We performed simulations at five temperatures, $T = 280, 300, 320, 340,$ and 360 K. For each temperature and for each solvent, we calculated the PMF from the average force exerted on each of the C_{60} 's.⁴⁹ Then, the average force acting between the two buckyballs along their axis of separation was integrated as a function of the distance between their centers of mass, d_{com} , to yield the Gibbs energy profile. The reaction coordinate, which was parallel to the z -axis, included 68 simulations with different values of d_{com} , ranging from 2.428 down to 0.908 nm. At each distance, the system was equilibrated for 2.0 ns, and subsequently, data were collected for an additional 12.0 ns. Because the PMF represents only relative values, it was shifted such that the Gibbs energy of the state at the largest separation corresponded to zero.

In order to achieve accurate analyses of the system (for both solvents at all temperatures) at the associated and dissociated

states, we performed additional simulations at each of these points for 240.0 ns. This was necessary because the change in enthalpy, which is approximated by the change in the potential energy of the system (justified by the negligible change in the volume of the system), is obtained by subtracting a large number from a similar large number. Because the positions of the solutes in our system were fixed, the entropy change of the system that we calculate equaled the unitary entropy, ΔS_u . Two water molecules were considered to be hydrogen-bonded if their oxygen–oxygen distance was smaller than 0.33 nm (the first minimum in the corresponding bulk RDF) and the donor–hydrogen–acceptor connectivity angle was larger than 150° .

RESULTS AND DISCUSSION

In Figure 1a, we display the change in Gibbs (free) energy for bringing two buckyballs from far apart into contact. As expected, the attractions (negative values of ΔG) are stronger in water than those in n -hexane. The magnitude of the attraction in water, $-17 < \Delta G < -14$ kJ/mol, is on the order of that between two benzene rings,¹⁰ and it increases with temperature. Previous studies of various hydrophobes in aqueous solution reported a minimum in the value of ΔG as a function of temperature^{25,28,29} and, in some cases, at much higher temperatures than those studied here. These Gibbs energies are decomposed into enthalpic and entropic parts in Figure 1b and c, respectively. Here, the behavior of the thermodynamic functions behaves completely different from those of other typical hydrophobic solutes. More specifically, in the association of two hydrophobic flat plates, ΔH is negative

for all temperatures and strongly and linearly decreases (i.e., increases in magnitude) with T .²⁵ This results in a large negative slope, indicating a large constant negative value of the heat capacity change at constant pressure, ΔC_p , which is characteristic of the hydrophobic interactions.¹¹ However, in the case of buckyball association, we find that ΔH is not strongly dependent on temperature (for $T > 320$, it is almost independent), implying a very small value for ΔC_p upon association. The curve of ΔH has a positive slope; the values are not all negative and change sign at around room temperature. The behavior of $T\Delta S$ is, correspondingly, also not a strong function of temperature. It is characterized by positive values with a positive slope, whereas in standard hydrophobic association in the large-scale regime, the values are also positive, however with a negative slope approaching zero at high temperature.^{20,25} Note that the values of $T\Delta S$ are larger than ΔH , and above room temperature, the entropy change is the only driving force for association. Not surprisingly, in hexane, both ΔH and $T\Delta S$ are even weaker functions of temperature, and also here, the attraction is driven only by entropy.

The induced PMFs in water at all temperatures, as a function of the distance between the centers of mass of the two buckyballs, d_{com} , are shown in Figure 1d. The equilibrium contact states occur at $d_{\text{com}} = 0.97$ nm (see Figure S2 (Supporting Information) for the location of the minima in the total PMF), and relative to the associated states at the largest distance, $d_{\text{com}} = 2.43$ nm, the induced contributions of the water molecules are repulsive (positive). Thus, the water molecules tend to push the two fullerenes apart. This solvent-induced repulsion decreases with temperature and almost vanishes at $T = 360$ K. In fact, the behavior at higher temperatures resembles more that of typical hydrophobic interactions in which there is a sharp decrease in the solvent-induced PMF for distances smaller than the last desolvation barrier, pushing the two solutes into contact. Nevertheless, even at the highest temperature, the value of the solvent-induced PMF of fullerenes is very large compared with that of graphene with a size of a benzene molecule.¹⁰ For the simulations in hexane, the contribution of the solvent-induced interactions to form the contact state is also only repulsive at all temperatures (Figure 1e).

Obviously, the direct interactions between the fullerenes allow the total PMF at contact to be negative despite the positive contribution from the solvent-induced interactions. The magnitude of this direct interaction between two C_{60} 's at contact is -18.5 kJ/mol, a value that is not large and can be even considered small when taking into account the number of carbon atoms involved. For example, the corresponding value for a graphene sheet with 28 carbons is -52.8 kJ/mol. Clearly, it is only the shape of the buckyballs that prevents stronger direct interactions (because in the contact state, there are only five carbon atoms from each fullerene that touch other carbons, whereas the other interatomic distances are larger). Thus, in contrast to previous reports in the literature, we argue that the negative values of ΔG for fullerene association in water arises despite the relatively weak, and not because of the strong, direct solute–solute interactions. In addition, it is the solvent-induced interaction between two fullerenes that accounts for their peculiar thermodynamic behavior. These interactions are composed of water–water and water–solute, and in order to investigate the role played by each one of them, we turn back to the change in enthalpy. In Figure 2, we decompose the change

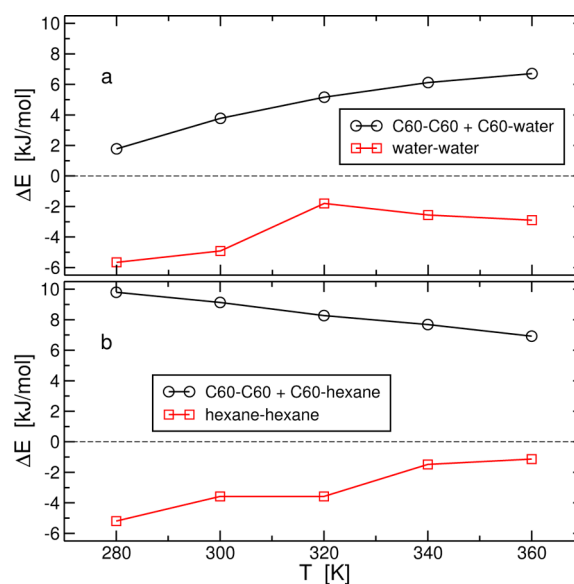


Figure 2. (a,b) Decomposition of the (total) change in enthalpy to the solvent–solvent (solvent reorganization) energy and to the sum of the solute–solute and solute–solvent energies for the simulations in water and hexane, respectively.

in ΔH (ΔE) into the solvent–solvent (solvent reorganization) and solvent–solute contributions. For the latter, we also added the solute–solute term. Nevertheless, even with that addition, the value of the sum of both terms is positive for all temperatures, which means that it opposes association. This means that the solute–solvent interactions lost upon dimerization are not compensated for by the direct solute–solute interactions. Results from scaled particle theory argue that this energetic term is responsible for the repulsive solvent-induced interaction⁵⁰). As for the solvent reorganization part, in both aqueous and nonpolar solvents, this energy term favors association. However, for water, the magnitude of this energy is small compared with that for two graphene sheets (in the large-scale regime), in which case the corresponding value is about -30 kJ/mol per 1 nm^2 buried surface area.¹⁰ It is worth mentioning that from this point of view, the buckyballs should be considered more as large-scale solutes because it seems that the waters around them cannot maintain the bulk hydrogen bond network (see also the inset of Figure 5).

Why is the solvent reorganization energy for C_{60} , having a diameter of about 1.1 nm, significantly smaller compared with that of a 28-atom graphene sheet with an exposed area of about 0.5 nm^2 ? In order to answer this question, we plot in Figure 3 the normalized density profile of the water molecules along the z -axis that reside inside of a cylinder with a cutoff radius, in the xy -plane, of 0.62 nm (centered along the line defined by the centers of mass of the two fullerenes). This was performed for the associated and dissociated states for three temperatures. On the basis of the behavior of these profiles, the waters are divided into bulk and interfacial (I1) waters. For the associated state, the latter is further divided into interfacial waters located at the surface farther away from the second fullerene (I1) and those that reside in between the two C_{60} 's (I2). In Figure 3, we define these different waters, in which I1 interfacial waters include the first two water layers from each of the fullerenes (see Figure 4 for snapshots depicting these waters). In the association process, some of the I1 interfacial waters are converted into I2 interfacial waters. The properties of the water molecules of

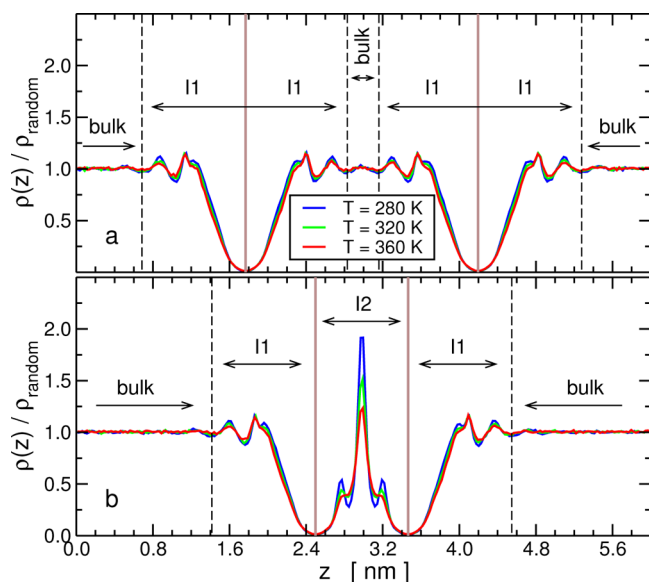


Figure 3. (a) The distribution of the water molecules (determined by the positions of the oxygen atoms) along the axis of approach of the two fullerenes (z -axis) for the dissociated state ($d_{\text{com}} = 2.428$ nm) at three different temperatures. The plots consider only waters inside of a cylinder with a radius, in the xy -plane, of 0.62 nm and centered along the line defined by the centers of mass of the two buckyballs. The two thick brown vertical lines mark the center of mass location of the two fullerenes, whereas the two dashed black lines, located 1.082 nm away from the fullerenes' centers of mass, distinguish bulk waters from interfacial waters (I1) with a thickness of two water layers. (b) Same as (a) but for the associated state ($d_{\text{com}} = 0.968$ nm). In this associated state, the waters residing between the two buckyballs introduce another type of interfacial waters (I2).

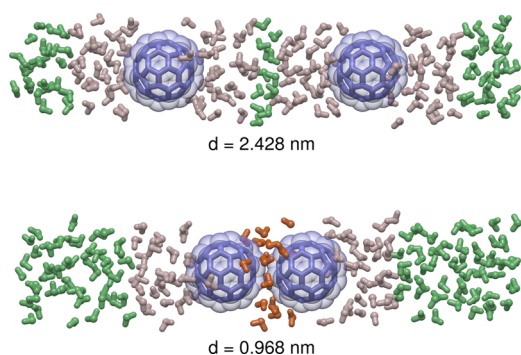


Figure 4. Cylindrical cuts around the buckyballs of the systems shown in the snapshots of Figure S1 (Supporting Information) ($d = d_{\text{com}}$). The three types of water molecules, using the same cutoff values defined in Figure 3, are shown in different colors, bulk in green, I1 in beige, and I2 in orange. Note that the process of bringing the two C_{60} 's from far apart into contact is accompanied by the transformation of some interfacial I1 waters into bulk waters and interfacial I2 waters.

the latter are distinct; they are trapped between two convex surfaces of the solutes and hence form a smaller number of hydrogen bonds with neighboring waters, compared with that formed by I1 waters, and as a consequence occupy a larger volume (smaller density).

The formation of interfacial waters I2 in the associated state, which are not present in the dissociated state, has several important consequences. In standard hydrophobic hydration, the interfacial waters (similar to I1 here) occupy a larger volume than bulk waters. Thus, when two hydrophobes come

into contact, there is a small reduction in the volume of the system (ΔV is negative), and this reduction increases in magnitude with temperature (i.e., exhibiting a negative slope).²⁵ However, in the case of buckyballs, ΔV is positive and exhibits a positive slope with temperature, as shown in Figure S3 (Supporting Information). The reason that ΔV is positive is due to the larger volume occupied by (i.e., the lower density of) interfacial waters I2 in the contact state relative to I1 and bulk waters. This lower density of I2 waters is observed despite their higher local density shown in Figure 3b. Furthermore, because the I2 waters are the most fragile waters in the system (they are engaged with the fewer number of hydrogen bonds), an increase in temperature will destabilize these waters the most, and eventually, they will transfer to the bulk phase (it is likely that I2 waters experience enhanced density fluctuations⁵¹). Thus, with a temperature increase, their number decreases, as seen in Figure 3b and computed explicitly in Figure S4 (Supporting Information), and as a consequence of this partial drying (or a decrease in the density of water), ΔV increases.

In Figure 5, we calculate the number of hydrogen bonds, per water molecule, for the three different waters in the associated

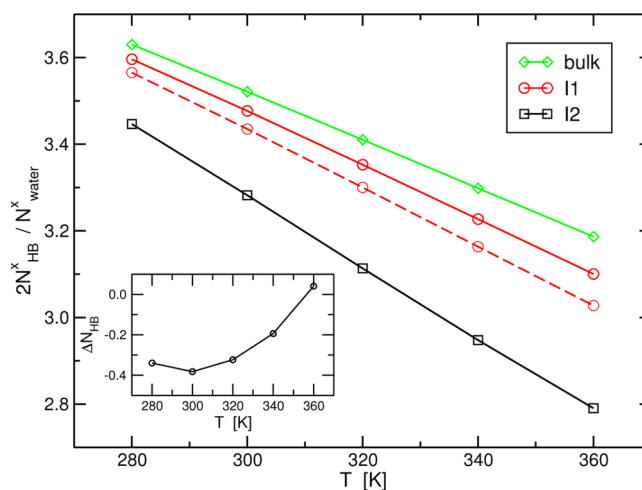


Figure 5. Average number of hydrogen bonds that a water molecule forms with its (water molecules) neighbors. The graph exhibits this number for the three different types of water molecules defined in Figure 3b for the contact state. The dashed red line is calculated for interfacial waters I1 when, alternatively, considering only the first layer away from the fullerene, thus using a cutoff distance of 0.736 nm from their center of mass. (Inset) The change of the total number of hydrogen bonds in the system for the association process calculated by eq 1.

state as a function of temperature. As expected, bulk waters form the largest number of hydrogen bonds. Next are the interfacial waters I1, which, in contrast to hydrophobic solvation at the small scale, display a smaller number of hydrogen bonds than bulk waters, confirming the assumption that buckyballs should not be viewed as small hydrophobic solutes. When considering only the first layer of waters away from the solutes, the linear line shifts down; thus, they form an even smaller number of hydrogen bonds. Interfacial waters I2 form the smallest number of hydrogen bonds, and the linear line is significantly smaller than that of I1 waters, independent of the number of layers defining the interface. In general, the differences in the number of hydrogen bonds formed by these different waters increase with temperature.

In Figure 1, we reported several abnormalities in the thermodynamics of fullerene association compared with that of typical hydrophobes. These can be understood by the conversion of some of the interfacial waters I1 to I2 waters upon dimerization. When two hydrophobic plates get into contact, there is a conversion of some of the interfacial waters to bulk waters; therefore, the total number of hydrogen bonds increases. However, here it is not clear that it would increase because the conversion of interfacial waters I1 also to I2 waters, and this particular conversion decreases the number of hydrogen bonds. Taking into account only the waters inside of the cylinder defined in Figure 3 and shown in Figure 4 (which is a very good assumption for calculating changes in the association process), we can estimate the change in the total number of hydrogen bonds in the system by

$$\begin{aligned} \Delta N_{\text{HB}} &= N_{\text{HB}}^{\text{associated}} - N_{\text{HB}}^{\text{dissociated}} \\ &= \frac{1}{2} [N_{\text{HB}}^{\text{I2}} N_{\text{I2}} + N_{\text{HB}}^{\text{bulk}} (N_{\text{I1}} - N_{\text{I2}}) - N_{\text{HB}}^{\text{I1}} N_{\text{I1}}] \end{aligned} \quad (1)$$

where in the expression after the last equality, N_X is the number of X waters in the associated state and N_{HB}^X is the number of hydrogen bonds per water molecule formed by X waters. The division by a factor of 2 is introduced to prevent double counting. The value of ΔN_{HB} as a function of temperature is plotted in the inset of Figure 5. It indicates a relatively small negative value for the total change in the number of hydrogen bonds that vanishes at the highest temperature. This explains the small enthalpy observed for the water reorganization energy in Figure 2a. In addition, the decrease in the density of I2 waters with temperature (partial drying) reduces the full-erence–water attraction energy at contact, yielding the positive slope shown for this curve in Figure 2a. Thus, with the sum of both terms, the small magnitude (that above room temperature has a positive value) and the positive slope of ΔH shown in Figure 1b can be understood.

In regard to the entropy change, the abnormal behavior is its small magnitude (for example, for a 28-atom graphene sheet, $T\Delta S = 51.8$ kJ/mol at room temperature) and its positive slope (in contrast to a negative one for typical hydrophobes). Figure 6 displays the normalized distributions of the orientations of the three different waters defined in Figure 3b for the two most extreme temperatures studied. The angle plotted is defined as the angle between the water dipole moment vector and the vector from the oxygen atom of the water to the center of mass of the closest buckyball. It is evident that I2 waters are more structured than I1 waters, whereas bulk waters are randomly oriented. The reduced sampling of the orientational space for the interfacial waters increases for lower temperatures. The smaller entropy of the I2 waters offsets the entropy gained from liberating to the bulk some of the I1 waters (as is normally the case with hydrophobe association) and, hence, the small magnitude of the net entropy change. Furthermore, the positive slope is also explained in this case by the decrease in the number of I2 waters with temperature (see Figure S4, Supporting Information), which decreases their negative contribution to the total entropy change.

Considering the association of two C_{60} 's in water, the repulsive solvent-induced interactions as well as the thermodynamic functions and their temperature dependence are in contrast to those observed for typical hydrophobes. We identify the presence of I2 interfacial waters in the dimeric state as the factor responsible for these peculiarities. The existence of the I2

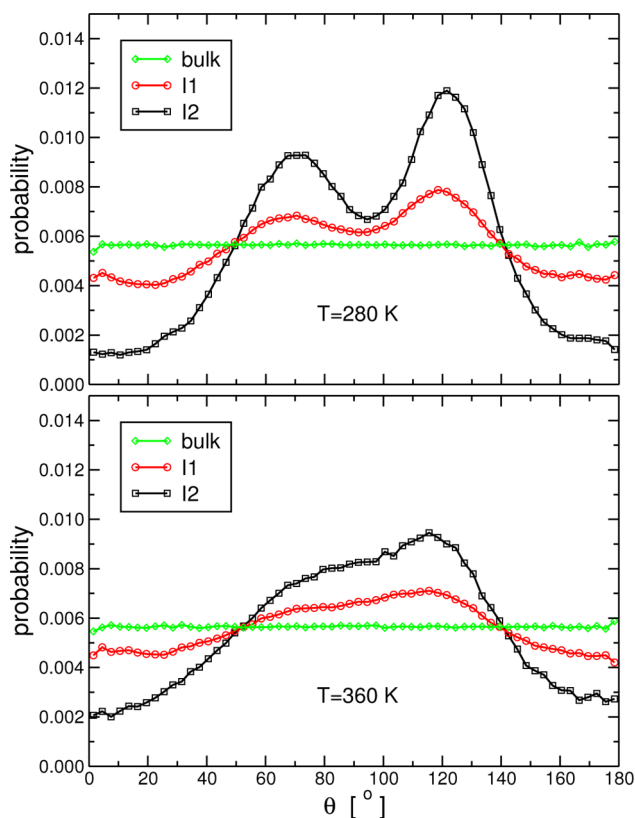


Figure 6. Normalized distributions of the orientations of the three different types of water molecules defined in Figure 3b at $T = 280$ (top panel) and 360 K (lower panel). The angle θ is defined as the angle between the dipole moment vector of a water molecule and the vector from the oxygen of this water to the center of mass of the closest fullerene. The intensity observed for θ is normalized by the cone angle $\sin \theta$.

waters is solely a result of the spherical shape of the buckyball and its size relative to that of a water molecule. For much smaller spherical solutes (e.g., methane molecules), the space between the two convex surfaces formed at contact is too small to accommodate water molecules; thus, I2 waters do not exist.

Going back to the question asked at the title: are buckyballs hydrophobic? It is clear that buckyballs do not display hydrophobic pairwise interaction; however, as far as solvation properties are concerned, they are hydrophobic. The latter includes both the hydration free energy of a single solute as well as solubility at the macroscopic scale. In the case of solvating a single C_{60} , no I2 interfacial waters exist, and we conjecture that the abnormalities due to the contact state will not be observed. On the macroscopic scale, the large aggregated state of the solute includes many pair interactions; nevertheless, the I2 waters will be stable only in the spaces between the C_{60} 's located at the interface with the water phase. The number of these I2 waters relative to the number of I1 waters liberated to the bulk will be too small to affect the macroscopic solvation properties. Thus, at the interior of the large C_{60} aggregate, the vacancies between the solute spheres will be dry and contribute to the hydrophobic nature of the buckyballs. As support for this argument, we note that differential calorimetric measurements reported a large negative value for the change in the heat capacity at constant pressure upon aggregation of fullerene derivatives of alanine and serine in aqueous solution.⁵² Therefore, it seems that buckyballs are one example in which

the effective pair interaction exhibits different qualitative behavior than the solubility. The origin of this difference is the character of the contact state that introduces qualitatively different interfacial waters in addition to the interfacial waters present in the dissociated state.

CONCLUSIONS

In this paper, we conducted MD simulations to address the observation that water molecules tend to push apart two buckyballs. Considering that these solutes are nonpolar and exhibit low solubility in water, this observation contradicts our concept of hydrophobicity in which waters push hydrophobic solutes toward each other. In addition to these repulsive solvent-induced interactions, we find that the associated changes in enthalpy and entropy and their temperature dependence contradict the behavior typical for hydrophobic interaction. The reason for this abnormal behavior is demonstrated to be the existence of waters in the space between the two convex surfaces of C_{60} fullerenes at contact (I2 interfacial waters). These waters are more orientated (i.e., smaller entropy), occupy a larger volume, and form a smaller number of hydrogen bonds compared with interfacial waters (I1) around the individually solvated fullerenes. We argue that despite the absence of hydrophobic character for the effective pair interaction, the solvation properties are hydrophobic. This is obvious for the hydration of a single C_{60} because only I1 interfacial waters exist. For the macroscopic case, the relative number of I2 waters (compared with the number of I1 waters liberated to the bulk) is small, which is likely to diminish their effect significantly. Thus, pairwise effective interactions are not always a mirror for solvation properties. More specifically, one cannot always assume pairwise hydrophobic interactions for solutes that exhibit hydrophobic solvation. However, it is possible to conclude on the nature of the pair interaction from solvation for cases in which the contact state can be extrapolated from the dissociated state. Comparing these results with those obtained for graphene sheets for which the solvent-induced interaction in water is attractive, we refute the argument that repulsive water-induced interactions are characteristic for all carbon nanoparticles.⁵³

Are the results presented in this work relevant for other solutes? As far as we can say, they are relevant to any hydrophobe forming a contact state with clefts that can host water molecules. It is likely that these waters will be characterized by a smaller number of hydrogen bonds compared with that of the interfacial waters around the individually hydrated solutes. As a consequence, similar abnormal behavior in the effective pair interaction is expected. For example, in the association of two carbon nanotubes along the line perpendicular to their long axes, the water-induced contribution was calculated to be repulsive.^{54,55}

ASSOCIATED CONTENT

Supporting Information

Snapshots of the simulation box and a few additional figures. The latter includes the total PMF, ΔV , and the number of I2 waters as a function of temperature. This material is available free of charge via the Internet at <http://pubs.acs.org>.

AUTHOR INFORMATION

Corresponding Author

*E-mail: r.zangi@ikerbasque.org.

Notes

The authors declare no competing financial interest.

ACKNOWLEDGMENTS

This work has been funded with support from the Basque Government under the SAIOTEK program, Project Code S-PE12UN014, and from the European Commission, Marie Curie International Reintegration Grant, Project Number 247485. Technical and human support provided by SGIker (USED SERVICES) (UPV/EHU, MICINN, GV/EJ, ESF) is gratefully acknowledged.

REFERENCES

- (1) Ruoff, R. S.; Tse, D. S.; Malhotra, R.; Lorents, D. C. Solubility of C_{60} in a variety of solvents. *J. Phys. Chem.* **1993**, *97*, 3379–3383.
- (2) Heymann, D. Solubility of C_{60} in alcohols and alkanes. *Carbon* **1996**, *34*, 627–631.
- (3) Richardson, C. F.; Schuster, D. I.; Wilson, S. R. Synthesis and characterization of water-soluble amino fullerene derivatives. *Org. Lett.* **2000**, 1011–1014.
- (4) Li, L.; Bedrov, D.; Smith, G. D. Repulsive solvent-induced interaction between C_{60} fullerenes in water. *Phys. Rev. E* **2005**, *71*, 011502.
- (5) Li, L.; Bedrov, D.; Smith, G. D. A molecular-dynamics simulation study of solvent-induced repulsion between C_{60} fullerenes in water. *J. Chem. Phys.* **2005**, *123*, 204504.
- (6) Makowski, M.; Czaplewski, C.; Liwo, A.; Scheraga, H. A. Potential of mean force of association of large hydrophobic particles: Toward the nanoscale limit. *J. Phys. Chem. B* **2010**, *114*, 993–1003.
- (7) Stillinger, F. H. Structure in aqueous solutions of nonpolar solutes from the standpoint of scaled-particle theory. *J. Solution Chem.* **1973**, *2*, 141–158.
- (8) Geiger, A.; Rahman, A.; Stillinger, F. H. Molecular dynamics study of the hydration of Lennard-Jones solutes. *J. Chem. Phys.* **1979**, *70*, 263–276.
- (9) Lum, K.; Chandler, D.; Weeks, J. D. Hydrophobicity at small and large length scales. *J. Phys. Chem. B* **1999**, *103*, 4570–4577.
- (10) Zangi, R. Driving force for hydrophobic interaction at different length-scales. *J. Phys. Chem. B* **2011**, *115*, 2303–2311.
- (11) Dill, K. A. The meaning of hydrophobicity. *Science* **1990**, *250*, 297.
- (12) Frank, H. S.; Evans, M. W. Free volume and entropy in condensed systems III. Entropy in binary liquid mixtures; partial molal entropy in dilute solutions; structure and thermodynamics in aqueous electrolytes. *J. Chem. Phys.* **1945**, *13*, 507–532.
- (13) Gill, S. J.; Wadsö, I. An equation of state describing hydrophobic interactions. *Proc. Natl. Acad. Sci. U.S.A.* **1976**, *73*, 2955–2958.
- (14) Muller, N. Search for a realistic view of hydrophobic effects. *Acc. Chem. Res.* **1990**, *23*, 23–28.
- (15) Kronberg, B.; Costas, M.; Silveston, R. Thermodynamics of the hydrophobic effect in surfactant solutions — micellization and adsorption. *Pure Appl. Chem.* **1995**, *67*, 897–902.
- (16) Lüdemann, S.; Abseher, R.; Schreiber, H.; Steinhauser, O. The temperature-dependence of hydrophobic association in water. pair versus bulk hydrophobic interactions. *J. Am. Chem. Soc.* **1997**, *119*, 4206–4213.
- (17) Paschek, D. Temperature dependence of the hydrophobic hydration and interaction of simple solutes: An examination of five popular water models. *J. Chem. Phys.* **2004**, *120*, 6674–6690.
- (18) Zangi, R.; Hagen, M.; Berne, B. J. Effect of Ions on the Hydrophobic Interaction between Two Plates. *J. Am. Chem. Soc.* **2007**, *129*, 4678–4686.
- (19) Zangi, R.; Engberts, J. B. F. N. Physisorption of hydroxide ions from aqueous solution to a hydrophobic surface. *J. Am. Chem. Soc.* **2005**, *127*, 2272–2276.
- (20) Baldwin, R. L. Temperature dependence of the hydrophobic interaction in protein folding. *Proc. Natl. Acad. Sci. U.S.A.* **1986**, *83*, 8069–8072.

- (21) Edsall, J. T. Apparent molal heat capacities of amino acids and other organic compounds. *J. Am. Chem. Soc.* **1935**, *57*, 1506–1507.
- (22) Eley, D. D. On the solubility of gases. Part I — The inert gases in water. *Trans. Faraday Soc.* **1939**, *35*, 1281–1293.
- (23) Eley, D. D. On the solubility of gases. Part II — A comparison of organic solvents with water. *Trans. Faraday Soc.* **1939**, *35*, 1421–1432.
- (24) Paschek, D. Heat capacity effects associated with the hydrophobic hydration and interaction of simple solutes: A detailed structural and energetical analysis based on molecular dynamics simulations. *J. Chem. Phys.* **2004**, *120*, 10605–10617.
- (25) Zangi, R.; Berne, B. J. Temperature dependence of dimerization and dewetting of large-scale hydrophobes: A molecular dynamics study. *J. Phys. Chem. B* **2008**, *112*, 8634–8644.
- (26) Blokzijl, W.; Engberts, J. B. F. N. Hydrophobic effects. opinions and facts. *Angew. Chem., Int. Ed. Engl.* **1993**, *32*, 1545–1579.
- (27) Privalov, P. L.; Gill, S. J. Stability of protein structure and hydrophobic interaction. *Adv. Protein Chem.* **1988**, *39*, 191–234.
- (28) Guillot, B.; Guissani, Y. A computer simulation study of the temperature dependence of the hydrophobic hydration. *J. Chem. Phys.* **1993**, *99*, 8075–8094.
- (29) Garde, S.; Hummer, G.; García, A. E.; Paulaitis, M. E.; Pratt, L. R. Origin of entropy convergence in hydrophobic hydration and protein folding. *Phys. Rev. Lett.* **1996**, *77*, 4966–4968.
- (30) Ray, C.; Brown, J. R.; Akhremitchev, B. B. Single-molecule force spectroscopy measurements of “hydrophobic bond” between tethered hexadecane molecules. *J. Phys. Chem. B* **2006**, *110*, 17578–17583.
- (31) Kauzmann, W. Some factors in the interpretation of protein denaturation. *Adv. Protein Chem.* **1959**, *14*, 1–63.
- (32) Nemethy, G.; Scheraga, H. A. Structure of water and hydrophobic bonding in proteins. II. Model for the thermodynamic properties of aqueous solutions of hydrocarbons. *J. Chem. Phys.* **1962**, *36*, 3401–3417.
- (33) Gill, S. J.; Dec, S. F.; Olofsson, G.; Wadsoe, I. Anomalous heat capacity of hydrophobic solvation. *J. Phys. Chem.* **1985**, *89*, 3758–3761.
- (34) Dill, K. A. Dominant forces in protein folding. *Biochemistry* **1990**, *29*, 7133–7155.
- (35) Wallqvist, A.; Berne, B. J. Computer simulation of hydrophobic hydration forces on stacked plates at short range. *J. Phys. Chem.* **1995**, *99*, 2893–2899.
- (36) Huang, X.; Margulis, C. J.; Berne, B. J. Dewetting-induced collapse of hydrophobic particles. *Proc. Natl. Acad. Sci. U.S.A.* **2003**, *100*, 11953–11958.
- (37) Choudhury, N.; Pettitt, B. M. On the mechanism of hydrophobic association of nanoscopic solutes. *J. Am. Chem. Soc.* **2005**, *127*, 3556–3567.
- (38) Hotta, T.; Kimura, A.; Sasai, M. Fluctuating hydration structure around nanometer-size hydrophobic solutes. I. Caging and drying around C₆₀ and C₆₀H₆₀ spheres. *J. Phys. Chem. B* **2005**, *109*, 18600–18608.
- (39) Wallqvist, A.; Berne, B. J. Molecular dynamics study of the dependence of water solvation free energy on solute curvature and surface area. *J. Phys. Chem.* **1995**, *99*, 2885–2892.
- (40) Werder, T.; Walther, J.; Jaffe, R.; Halicioglu, T.; Koumoutsakos, P. On the water–carbon interaction for use in molecular dynamics simulations of graphite and carbon nanotubes. *J. Phys. Chem. B* **2003**, *107*, 1345–1352.
- (41) Hess, B.; Kutzner, C.; van der Spoel, D.; Lindahl, E. GROMACS 4: Algorithms for highly efficient, load-balanced, and scalable molecular simulation. *J. Chem. Theory Comput.* **2008**, *4*, 435–447.
- (42) Darden, T.; York, D.; Pedersen, L. Particle mesh Ewald: An N-log(N) method for Ewald sums in large systems. *J. Chem. Phys.* **1993**, *98*, 10089–10092.
- (43) Bussi, G.; Donadio, D.; Parrinello, M. Canonical sampling through velocity rescaling. *J. Chem. Phys.* **2007**, *126*, 014101.
- (44) Berendsen, H. J. C.; Postma, J. P. M.; van Gunsteren, W. F.; DiNola, A.; Haak, J. R. Molecular dynamics with coupling to an external bath. *J. Chem. Phys.* **1984**, *81*, 3684–3690.
- (45) Horn, H. W.; Swope, W. C.; Pitera, J. W.; Madura, J. D.; Dick, T. J.; Hura, G. L.; Head-Gordon, T. Development of an improved four-site water model for biomolecular simulations: TIP4P-Ew. *J. Chem. Phys.* **2004**, *120*, 9665–9678.
- (46) Miyamoto, S.; Kollman, P. A. SETTLE: An analytical version of the SHAKE and RATTLE algorithms for rigid water models. *J. Comput. Chem.* **1992**, *13*, 952–962.
- (47) Schuler, L.; van Gunsteren, W. F. On the choice of dihedral angle potential energy functions for n-alkanes. *Mol. Sim.* **2000**, *25*, 301–319.
- (48) Hess, B.; Bekker, H.; Berendsen, H. J. C.; Fraaije, J. G. E. M. LINCS: A linear constraint solver for molecular simulations. *J. Comput. Chem.* **1997**, *18*, 1463–1472.
- (49) Paladino, A.; Zangi, R. Ribose 2'-hydroxyl groups stabilize RNA hairpin structures containing GCUAA pentaloop. *J. Chem. Theory Comput.* **2013**, *9*, 1214–1221.
- (50) Graziano, G. On the pairwise hydrophobic interaction of fullerene. *Chem. Phys. Lett.* **2010**, *499*, 79–82.
- (51) Jamadagni, S. N.; Godawat, R.; Garde, S. Hydrophobicity of proteins and interfaces: Insights from density fluctuations. *Annu. Rev. Chem. Biomol. Eng.* **2011**, *2*, 147–171.
- (52) Danilenko, A. N.; Romanova, V. S.; Kuleshova, E. F.; Parnes, Z. N.; Braudo, E. E. Heat capacities of aqueous solutions of amino acid and dipeptide derivatives of fullerene. *Russ. Chem. Bull.* **1998**, *47*, 2134–2136.
- (53) Li, L.; Bedrov, D.; Smith, G. D. Water-induced interactions between carbon nanoparticles. *J. Phys. Chem. B* **2006**, *110*, 10509–10513.
- (54) Uddin, N. M.; Capaldi, F. M.; Farouk, B. Molecular dynamics simulations of the interactions and dispersion of carbon nanotubes in polyethylene oxide/water systems. *Polymer* **2011**, *52*, 288–296.
- (55) Ou, S.; Patel, S.; Bauer, B. A. Free energetics of carbon nanotube association in pure and aqueous ionic solutions. *J. Phys. Chem. B* **2012**, *116*, 8154–8168.